as much as a billion years or more for the martian groundwater system to achieve hydrostatic equilibrium, and the ~2–4 km elevation difference between the outflow channel source regions and the northern plains, the water confined beneath the frozen crust of the northern plains should have been under a significant hydraulic head. Thus, the existence of a hydraulic pathway between the ponded flood waters above the northern plains and the confined aquifer lying beneath it would not have led to the infiltration of flood water back into the crust, but rather the additional expulsion of groundwater onto the surface.

A more detailed discussion of the fate of flood waters discharged by the martian outflow channels is currently in preparation.

References: [1] Clifford S. M. (1993) *JGR, 98,* 10973–11016. [2] Carr M. H. (1979) *JGR, 84,* 2995–3007. [3] Brace W. F. (1980) *Int. J. Rock Mech. Min. Sci. Geochem. Abstr., 17,* 241–251.

REGIONAL SEDIMENTOLOGICAL VARIATIONS AMONG DARK CRATER FLOOR FEATURES: TOWARD A MODEL FOR MODERN EOLIAN SAND DISTRIBUTION ON MARS.

K. S. Edgett and P. R. Christensen, Department of Geology, Arizona State University, Tempe AZ 85287-1404, USA.

It has been known since 1972 that many martian craters (≤ 25 km diameter) have dark features on their floors, and that when seen at higher image resolution, some of the dark units are dune fields [1–3]. Interpretations of thermal inertia derived from Viking Infrared Thermal Mapper (IRTM) data have been used to suggest that many dark intracrater features, including those where dunes are not observed in images, contain some amount of sand or particles in the range 0.1–10 mm [4,5]. However, it has never been known if all these dark features consist of dunes.

We assembled a set of 108 carefully constrained Viking IRTM observations for dark crater-floor units. The data and selection criteria are described in detail elsewhere [6–9]. Studied in conjunction with Mariner 9 and Viking orbiter images of each crater, these data indicate that the dark crater-floor units in some regions have different thermal properties than those in other regions [7–9]. Figure 1 shows thermal inertia means and standard deviations for dark intracrater units in nine different regions. Thermal inertias were computed using the Viking thermal model of H. H. Kieffer and corrected for atmospheric CO_2 effects using the relationship for a dust-free atmosphere shown by Haberle and Jakosky [10]. The thermal inertias and interpreted particle sizes in Fig. 1 are regarded as upper limits, with lower limits (due to suspended dust in the atmosphere) perhaps 50–200 J m^{-2} s$^{-0.5}$ K^{-1} less than shown [10,11]. However, because the atmosphere had a nearly uniform dust opacity from L_s 344°–125° over the regions examined [12], the relative differences between regions in Fig. 1 are genuine [9].

The thermophysical differences illustrated in Fig. 1 [also see 7–9] are probably related to regional variations in the amount of surface covered by sand and perhaps dunes. In two of these regions, Hellespontus and Oxia, the thermal differences are consistent with an observed difference in the morphology of dunes comprising the dark features. In Hellespontus there are large transverse dunes while in Oxia there are fields of small barchans [2,9,13]. The regional differences are independent of the exact thermal inertia and particle size inferred for each, but sand (0.06–2 mm) is probably the dominant particle size [5,9,14].

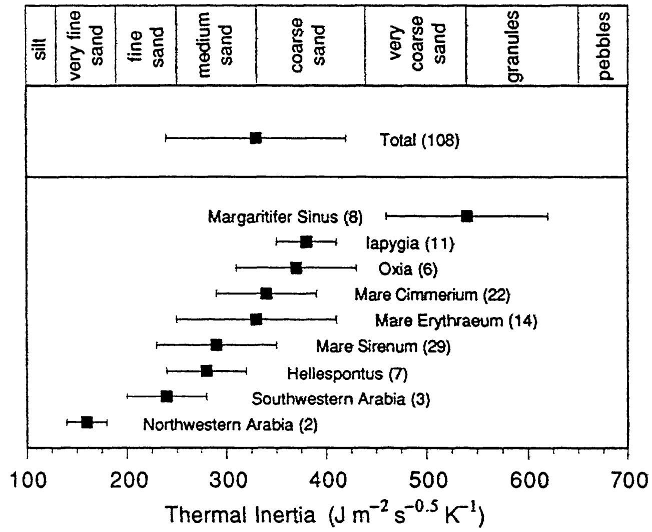

Fig. 1. Mean and standard deviation of thermal inertias for dark intracrater features in different regions. Numbers in parentheses indicate total craters examined. To convert thermal inertia to units of 10^{-3} cal cm^{-2} s$^{-0.5}$ K^{-1}, divide by 41.84.

In an unvegetated environment, the form and scale of eolian sand deposits are functions of sand availability, grain size distribution, wind energy and directional variability, the presence of topographic obstacles (e.g., crater walls), and climatic variations that might affect any of these factors [15]. In terms of sand-deposit morphology, grain size is probably not a significant control except among zibars [16]. Barchan and transverse dunes are typical of unidirectional wind regimes; their differences are largely considered a function of "sand supply": the amount of loose sand available for eolian transport in a region [17]. Barchans form in areas of low sand supply, though transverse dunes do not form exclusively in places of high sand supply [18]. Transverse dunes on Mars can be large deposits like those in Hellespontus or they can be small and difficult to identify without high-resolution images (an example occurs in Pettit Crater [19]).

To first order, the areal coverage of eolian sand (dunes, drifts, sheets) may be the main factor causing the observed regional differences in the thermal properties of low-albedo intracrater units [8,9]. The percentage of dune cover [8] may be similar among craters within a given region, but different between regions. The amount of sand transported and deposited is likely related to two main factors: sand supply and wind regime.

Sand sources that are regional in extent might include pyroclastic deposits laid down over a vast area, or perhaps fluvial and lacustrine strata. Detection of such sources will require high-resolution imaging or investigation on the planet's surface to find deposits or outcrops of volcaniclastic or fluviolacustrine sandstones from which dark sand might have eroded. Location of sand sources will also require remote multispectral observations to determine the mineralogy of the sediment and to trace wind-worked sand back to source areas.

Regional wind regimes are important because the wind distributes sand over an area, removes material from a source, and forms deposits such as dunes. Sand has been or is being distributed in the classical albedo regions of Mars in different ways. In Hellespontus, for example, there appears to be a considerable volume of sand present, but it is entirely piled up into large transverse dunes. In Hellespontus, there appears to be little dark material that is not piled up in dunes. This is in contrast with craters in low-albedo regions like Mare Cimmerium or Margaritifer Sinus, where there are many extracrater dark deposits. The configuration of dunes in Hellespontus might have resulted from winds that were strong enough to strip loose sand from the surrounding areas and deposit the sand in craters.

In contrast, some of the sand from small barchans in Oxia has been removed from the craters to form dark streaks [20]. In places, the streaks coalesce to make larger, low-albedo units like Oxia Palus (9°N, 16°W). Barchans indicate that the amount of loose sand available for transport in Oxia is small relative to Hellespontus, yet the winds might have been more vigorous in order to facilitate the movement of sand in and out of craters and prevent the accumulation of fine, bright dust over the whole region. The coalescence of dark streaks forming Oxia Palus may provide a model for the formation of low-albedo regions like Mare Cimmerium, Mare Sirenum, or Margaritifer Sinus, where the winds may be stronger [21] and the sand supply might be greater than in Oxia, thus causing sand to be more widely distributed. Alternatively, the sources of sand in low-albedo regions might be more ubiquitous. Perhaps sediment beds are currently eroding and feeding the present-day dark eolian deposits found throughout the low-albedo regions.

Which of the two influences, broadly termed "wind regime" and "sand supply," has had the greatest influence on the nature of eolian sediment deposition and removal in different martian regions remains to be understood. One additional factor is the question of climatic change; for example, were the huge piles of sand in the Hellespontus craters deposited under climate conditions that were different from the present?

References: [1] Sagan C. et al. (1972) *Icarus, 17*, 346–372. [2] Cutts J. A. and Smith R. S. U. (1973) *JGR, 78*, 4139–4154. [3] Arvidson R. E. (1974) *Icarus, 21*, 12–27. [4] Peterfreund A. R. (1981) *Icarus, 45*, 447–467. [5] Christensen P. R. (1983) *Icarus, 56*, 496–518. [6] Edgett K. S. (1990) M.S. thesis, Arizona State Univ. [7] Edgett K. S. and Christensen P. R. (1991) *LPSC XXII*, 335–336. [8] Edgett K. S. and Christensen P. R. (1992) *LPSC XXIII*, 325–326. [9] Edgett K. S. and Christensen P. R. (1993) *JGR*, submitted. [10] Haberle R. M. and Jakosky B. M. (1991) *Icarus, 90*, 187–204. [11] Paige D. A. et al. (1993) *JGR*, submitted. [12] Martin T. Z. and Richardson M. I. (1993) *JGR, 98*, 10941–10949. [13] Thomas P. (1984) *Icarus, 57*, 205–227. [14] Edgett K. S. and Christensen P. R. (1991) *JGR, 96*, 22765–22776. [15] Pye K. and Tsoar H. (1990) *Aeolian Sand and Sand Dunes*, 218–220, Unwin and Hyman, London. [16] Lancaster N. (1989) *The Namib Sand Sea*, 111–112, A. A. Balkema, Rotterdam. [17] Wasson R. J. and Hyde R. (1983) *Nature, 304*, 337–339. [18] Rubin D. M. (1984) *Nature, 309*, 91–92. [19] Zimbelman J. R. (1986) *Icarus, 66*, 83–93. [20] Thomas P. et al. (1981) *Icarus, 45*, 124–153. [21] Greeley R. et al. (1993) *JGR, 98*, 3183–3196.

AEROSOLS SCATTERING AND NEAR-INFRARED OBSERVATIONS OF THE MARTIAN SURFACE. S. Erard, IAS-Planetologia, viale dell'Universita 11, 00185 Roma, Italy.

Introduction: The presence of a scattered contribution in the atmosphere of Mars is a major problem for spectroscopic observations of the surface in the infrared since the main mineralogical absorptions have a typical depth of 1% and could be easily masked or subdued by atmosphere scattering. An estimate of the aerosol contribution between 0.77 and 2.6 μm was previously derived above Tharsis from ISM imaging spectroscopic data acquired from the Phobos 2 spacecraft in 1989 [1]. It is used here to investigate the effect of the scattering on the criteria that allow the mineralogical characterization of the surface.

Aerosols Contribution: Under low opacity and near-normal viewing geometry (the conditions of ISM observations) multiple atmospheric scattering can be neglected. Because the martian aerosols are very bright and strongly forward-scattering in the near-IR, the radiance factor can be further approximated as the sum of the surface reflectance and the backscattering [2]. This model was used to derive an estimate of the scattered spectrum, taking advantage of the overlap between two image cubes in the region of Pavonis Mons

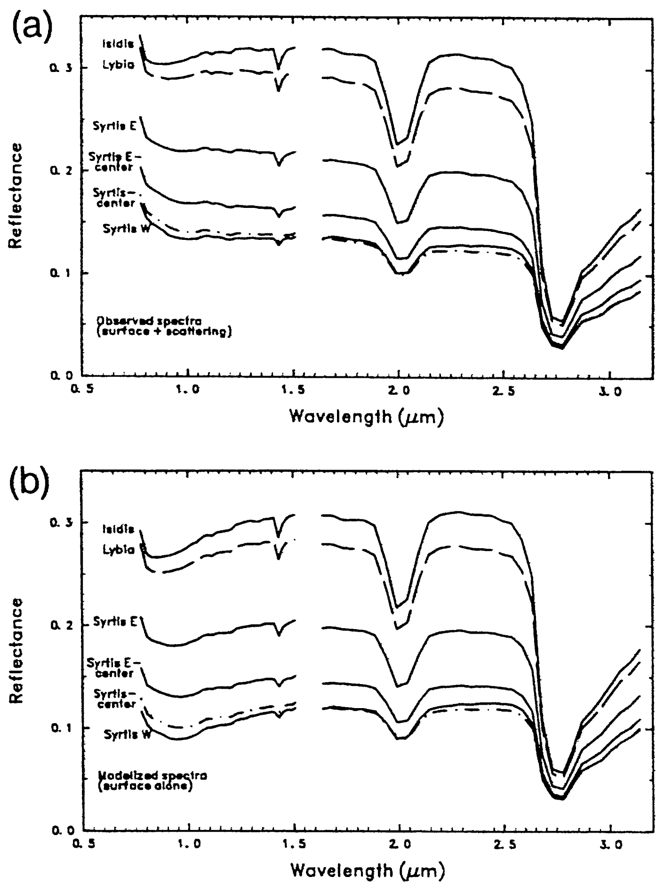

Fig. 1. Average spectra of the six main spectral units in the Syrtis Major-Isidis Planitia image-cube: **(a)** calibrated spectra; **(b)** after removal of the estimated scattering.